Astronomy & Astrophysics manuscript no. FinalPaper
March 5, 2014

Collision Avoidance in Next-generation Fiber Positioner Robotic Systems for Large Survey Spectrographs

Laleh Makarem[1,7], Jean-Paul Kneib[2,3], Denis Gillet[1], Hannes Bleuler[4], Mohamed Bouri[4], Laurent Jenni[4], Francisco Prada[5,6], and Justo Sanchez[5]

[1] Coordination and Interaction Systems Group (REACT), Ecole Polytechnique Fédérale de Lausanne (EPFL), Switzerland
[2] Laboratory of Astrophysics (LASTRO), Ecole Polytechnique Fédérale de Lausanne (EPFL), Observatoire de Sauverny, Ch-1290 Versoix, Switzerland
[3] Aix Marseille Université, CNRS, LAM (Laboratoire d'Astrophysique de Marseille) UMR 7326, 13388, Marseille, France
[4] Laboratory of Robotic Systems (LSRO) Ecole Polytechnique Fédérale de Lausanne (EPFL), Switzerland
[5] Instituto de Astrofisica de Andalucia (CSIC), Granada, E-18008, Spain
[6] Instituto de Física Teórica, (UAM/CSIC), Universidad Autónoma de Madrid, Cantoblanco, E-28049 Madrid, Spain
[7] e-mail: laleh.makarem@epfl.ch

March 5, 2014

ABSTRACT

Some of the next generation massive spectroscopic survey projects, plan to use thousands of fiber positioner robots packed at a focal plane to quickly move in parallel the fiber-ends from the previous to the next target points. The most direct trajectories are prone to collision that could damage the robots and impact the survey operation. We thus present here a motion planning method based on a novel decentralized navigation function for collision-free coordination of fiber positioners. The navigation function takes into account the configuration of positioners as well as the actuator constraints. We provide details for the proof of convergence and collision avoidance. Decentralization results in linear complexity for the motion planning as well as dependency of motion duration with respect to the number of positioners. Therefore the coordination method is scalable for large-scale spectrograph robots. The short in-motion duration of positioner robots, will thus allow the time dedicated for observation to be maximized.

Key words. astronomical instrumentation, methods and techniques; instrumentation: spectrographs; surveys; collision avoidance; motion control; multi agent robotics; collective motion planning; decentralized navigation function

Use \titlerunning to supply a shorter title and/or \authorrunning to suply a shorter list of author.

1. Introduction

After the discovery and confirmation of the accelerated expansion of the universe (Riess et al. 1998; Perlmutter et al. 1999), one of the main challenges in cosmology is to discern the nature of the dark energy. In order to achieve this goal, different observational techniques have been proposed to tackle the geometry and evolution of the Universe. One of the key techniques is the measurement of the Baryonic Acoustic Oscillations (BAO) in massive spectroscopic surveys.

The very first large-scale spectroscopic survey (Huchra et al. 1983) revealed a cosmic web structure with filaments and voids, and soon after, further investigations questioned the existence of a cosmological constant (Efstathiou et al. 1990). More recently, following the discovery of the imprint of the BAO in the Sloan Digital Sky Survey (SDSS; Eisenstein et al. 2005), massive spectroscopic surveys have been developed to measure accurately the evolution of the distance-redshift relation using the BAO technique. In particular, 1) the WiggleZ redshift survey (Blake et al. 2011) has completed a ∼250,000 redshift survey of star-forming galaxies (at $z < 0.8$) at the 4m Anglo Australian Telescope (AAT), 2) the Baryonic Oscillation Spectroscopic Survey (BOSS; Anderson et al. 2012) will complete in 2014 a major redshift survey of 1.4 million galaxy redshift (at $z < 0.7$) and 160,000 high-redshift Lyman-α quasars using the SDSS telescope, and 3) the extended-BOSS survey (2014-2020) will complete the first BAO survey over the redshift range $0.7 < z < 2.2$ using galaxies and quasars as well as the SDSS facility.

To go beyond the throughput limits of current surveys, new technologies are being developed to hasten the future spectroscopic facilities. The way forward is not only to use larger aperture telescopes, but also to use a larger multiplexing. Over the past few years two major projects have been approved for construction. First, the Primary Focus Spectrograph (PFS) is a Japanese lead project that aims to develop a 2400-fiber spectrograph on the 8.2 m Subaru telescope. Second, the Dark Energy Spectroscopic Instrument (DESI)[1], a DOE lead project, aims to develop a 5000-fiber spectrograph on the Mayall 4m telescope. Other less advanced projects are also being prepared such as 4MOST and WEAVE.

Spectrographs fed by massive fiber bundles are one of the most advanced and proven methods compared with multi-slit approach. Various technologies have been proposed for fiber positioning. For example, in the case of the SDSS spectrograph, fibers are placed manually into the holes drilled in an aluminum plate. This operation is done during the day time prior to observations. In the case of the AAT spectrograph a robot places fibers one at a time at the target points. This operation is done while another set of fiber is observing. In the case of the Chinese Large Sky Area Multi-Object Fibre Spectroscopic Tele-

[1] http://desi.lbl.gov

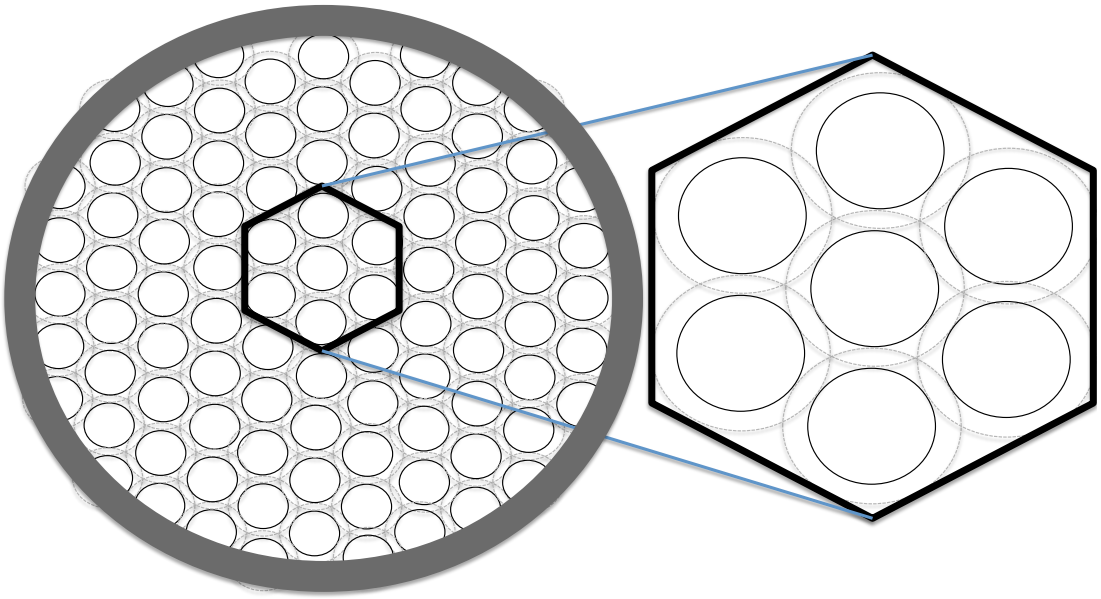

Fig. 1. Configuration of robot positioner on a focal plane. Positioners shown as black circles, form a hexagonal array in order to cover a patrol disc (shown in a dashed gray circle) as versatile as possible.

scope (LAMOST; Cui et al. 2010), and the Japanese Fibre Multi-Object Spectrograph (FMOS; Kimura et al. 2003) robotic fiber positioners are placing in parallel the fibers at the target points just before the observations are conducted. The key advantage of using robotic positioners is that the fibers could be positioned simultaneously. So if the robotic system is fast, reconfiguration time could executed during the observation overheads (readout time of the detectors and slewing of the telescope).

In the next-generation fibre-fed spectrographs such as DESI and PFS projects, small robots are responsible to position the fiber-ends. In order to improve the versatility of the system and ensure the maximum number of observed galaxies the robots share working spaces. Both project will use a robot with two degrees of freedom and eccentric rotary joints (so called $\theta-\phi$ design). Our initial motivation for taking $\theta-\phi$ design as an example for this paper, undertaken as part of DESI project, is to solve the collision challenge in motion planning of these robots. The proposed method could directly overcome the collision problem for any robot with two rotary joints that move a single fiber-end such as for the aforementioned DESI and PFS projects. This work presents a new motion planning method for the positioner robots based on Decentralized Navigation Functions (DNF). The proposed trajectories guarantee collision-free path for all the fiber-ends. The motion planning is decentralized in order to be able to extend the solution for large-scale positioner robots. In addition, the DNF method could be adopted for other fiber positioning systems with different geometry patterns in case they have potential risk of collision.

This paper is organized as follows. In section 2, a description of the focal plane is given. In section 3, we give the problem formulation for a collision-free trajectory planner. The solution to this problem, using DNF, is given in section 4. Proof of convergence and constraints on parameter tuning is explained in section 5. The simulation results corresponding to the proposed approach are presented and discussed in section 6. Section 7 briefly explores some avenues for future research and concludes.

2. Description of focal plane

We describe a standard design for the focal plane, which can be extended to a number of future fibre-fed multi-object spectrograph instruments (and particularly designs explored for DESI and PFS). The main concept is a collection of identical positioners distributed over an hexagonal array (See Fig. 1). Each positioner robot is therefore assigned to a single target or if no target is accessible will observe the sky. The positioner robots could cover the entire focal plane and each move a fibre head toward a desired location within the patrol disc of positioner. Because we require that any point of the focal plane is accessible by a fiber, there will be regions of the focal plane where the workspaces of adjacent positioners will overlap. In these overlap zones there is a risk of actuator collision. Target assignment and collision avoidance strategies will therefore be among the challenges in the design of such a massively parallel fibre-fed spectrograph.

2.1. Target assignment

Several strategies can be developed in order to assign targets - galaxies, quasars or stars- to the end effectors -fiber-ends- of the positioner robots. The simplest approach is to select randomly for each positioner any of the targets lying within the corresponding working space (patrol disc). To achieve an opti-

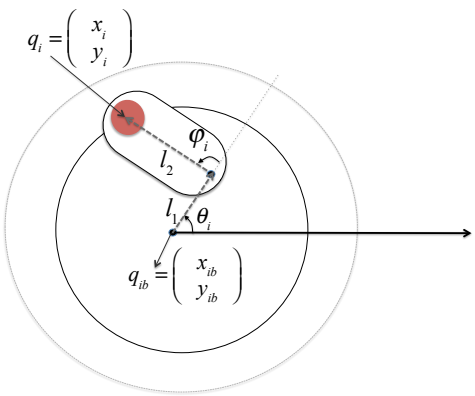

Fig. 2. A positioner robot with two degrees of freedom. The main disk (black circle) rotates along its central axis. Its angular position is shown as θ_i. The arm with the length of l_2 rotates around an eccentric axis (with the distance of l_1 from the center) fixed on the main disk and its angular position is shown as ϕ_i. q_{ib} is the position of the robot base fixed to the telescope structure in a global frame attached to the focal plane. q_i is the position of the fiber attached to the robot i in that global frame.

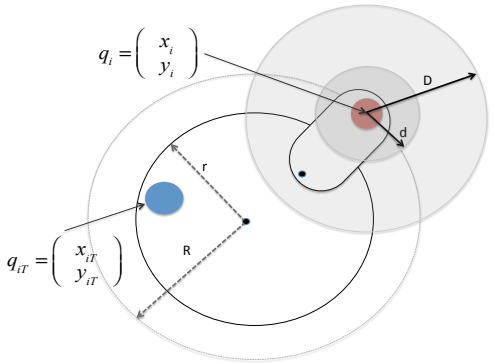

Fig. 3. The target point q_{iT} is the destination of the robot end-effector. The collision detection envelope with radius of D, is the area where collision avoidance term in the navigation function is activated. The collision avoidance term in the navigation function ensures that the two positioner end-effectors will keep a distance larger than d.

mal solution, which means that the maximum number of targets is observed during a certain period of time, the drain algorithm was introduced (Morales et al. 2012). The method ensures observation of maximum number of targets in the first few sets of observations. Using both randomly distributed targets and mock galaxy catalogues, the authors showed that the number of observed galaxies could be increased by 2 percents in the first set of observations.

In this paper we assume that target assignment has been effectively done by one of the mentioned algorithms under three main assumptions. First, each target is assigned to one positioner only, and each positioner is assigned to maximum one target. Second, the target assigned to each positioner is always within its patrol disc and hence reachable by the positioner. The minimum distance between two assigned targets is d. Thus, the focus of the work presented here is on the coordination of positioners in motion to avoid collision. We assume that the target of each positioner is fixed (not a quickly moving target) and known to the positioner robot.

3. Problem formulation

We consider a system composed of N positioner robots. The goal of each robot is to put its end effector (fiber-end) on an assigned target point. Each positioner is a planar robot with two degrees of freedom, each moving by a rotational motor (Fig. 2).

Each positioner robot covers the patrol area (workspace) through two correlated rotations: θ rotates around the actuator's main axis, while ϕ moves the fiber arm tip from the peripheral circle to the central axis (Fig. 2). The optical fiber is attached to a ferrule at the arm tip, and passes through the center of the actuator and exits by the rear side of the robot.

The forward kinematics of each positioner robot can be described as:

$$\begin{pmatrix} x_i \\ y_i \end{pmatrix} = \begin{pmatrix} x_{ib} \\ y_{ib} \end{pmatrix} + \begin{pmatrix} cos\theta_i & cos(\theta_i + \phi_i) \\ sin\theta_i & sin(\theta_i + \phi_i) \end{pmatrix} \begin{pmatrix} l_1 \\ l_2 \end{pmatrix} \quad (1)$$

Where the end-effector position of positioner i is $q_i = (x_i, y_i)$ in a global frame attached to the focal plane. l_1 and l_2 are first and second rotation links respectively (Fig. 2). θ and ϕ are angular positions of the two joints of the positioner i. Each positioner is controllable by its angular velocity, meaning the speed of each of the two motors.

The main challenge is to coordinate the robots in motion to reach a predefined target point while avoiding collisions. The proposed approach should be expandable to a more large-scale problems. A centralized solution for such a problem would be practically infeasible and costly due to the presence of numerous positioners and constraints (Tanner and Kumar 2005). Therefore, among all the methods found in the literature for coordinating agents, decentralized and reactive control approaches seem promising.

4. Decentralized Navigation Function

Inspired by the emergent behaviors among swarms (insects, birds, fishes), methods based on local reactive control have received great interest (Ge et al. 2012). Therefore, artificial potential fields are often exploited for the coordination of autonomous agents. The main drawback of most potential field approaches is that convergence to the target is not guaranteed due to the presence of spurious local minima. In order to solve this problem and present a complete exact solution for the coordination problem, navigation functions have been introduced (Dimarogonas and Kyriakopoulos 2005).

Navigation functions have been used in various robotic and control applications (Makarem and Gillet 2011, 2012; De Gennaro and Jadbabaie 2006). In these applications the actuation torque or other inputs (e.g., the acceleration, the velocity) is derived from some potential function that encodes relevant information about the environment and the objective. In the framework of the problem presented in this paper, the use of navigation functions in a decentralized scheme is promising, as it can be implemented in real-time and it also shows good flexibility with regard to adding new robots and changing the problem constraints.

A navigation function is practically a smooth mapping which should be analytic in the workspace of every positioner robot and its gradient would be attractive to its destination and repulsive

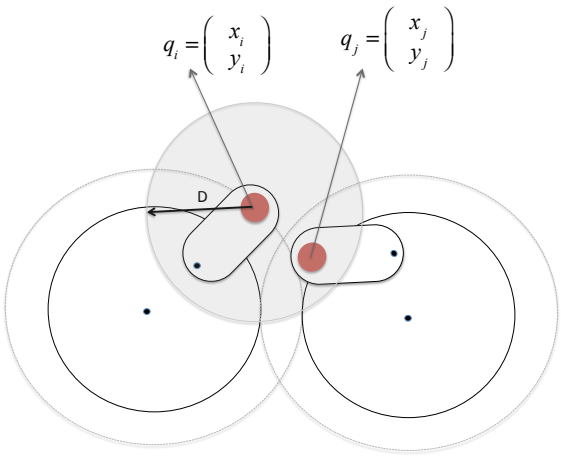

Fig. 4. A configuration in which there is a risk of collision between the end-effectors of two robots. In this configuration the collision avoidance term in the navigation functions of the two robots are active which means they take values more than zero.

from other robots. So, an appropriate navigation function could be combined with a proper control law in order to obtain a trajectory for every motor of the robot leading to the destination and avoiding collisions.

We propose a navigation function ψ_i for the positioner i in (2) which is composed of two components. The first term, the attractive component, is the squared distance of the end-effector of positioner robot i from its target point. This term of navigation function attains small values as the positioner brings the fiber closer to its target point (Fig. 3). The second term, the repulsive component, aims at avoiding collisions between positioner i and the six other positioners located in its vicinity. This term is activated when the two positioner robots are closer than a distance D, otherwise this term is zero. D defines the radius of a collision avoidance envelope and $d < D$ defines the radius of the safety region. The closer the two robots get, the higher values this repulsive term attains. Moving toward the minimum point of this navigation function will guarantee the minimum distance of d between the positioners (Fig. 4). λ_1 and λ_2 are the two weighting parameters related to the two terms in the navigation function.

$$\psi_i = \lambda_1 \left\| q_i - q_{iT} \right\|^2 + \lambda_2 \sum_{j \neq i} min(0, \frac{\left\| q_i - q_j \right\|^2 - D^2}{\left\| q_i - q_j \right\|^2 - d^2}) \tag{2}$$

According to the navigation function presented in (2) and the forward kinematics defined in (1), the following control law is proposed:

$$u_i = -\nabla_{\theta_i \phi_i} \psi_i(q_i) \tag{3}$$

At each step, the robot will move the fiber according to a gradient descent method. It is worth mentioning that, the navigation function is directly a function of the end-effector positions. In order to obtain the angular velocities of each of two motors, we calculate the gradient of the navigation function with respect to the angular positions of the links using the chain derivatives and the forward kinematics in (1).

$$\begin{pmatrix} \omega_{i1} \\ \omega_{i2} \end{pmatrix} = u_i = -\begin{pmatrix} \frac{\partial \psi_i}{\partial x_i}\frac{\partial x_i}{\partial \theta_i} + \frac{\partial \psi_i}{\partial y_i}\frac{\partial y_i}{\partial \theta_i} \\ \frac{\partial \psi_i}{\partial x_i}\frac{\partial x_i}{\partial \phi_i} + \frac{\partial \psi_i}{\partial y_i}\frac{\partial y_i}{\partial \phi_i} \end{pmatrix} \tag{4}$$

ω_{i1} and ω_{i2} are the angular velocity of the first and second motor of positioner robot i respectively. There could be two final configurations that result in the same target point. However, when traveling from a known configuration, reaching to one of those configurations is faster considering no collision. In this work we assumed that the faster configuration is the goal configuration.

4.1. Algorithm complexity

Table 1 describes the motion planning algorithm. In each time step dt, each positioner robot computes the speed of its two motors knowing its current position and the target point as well as the position of adjacent robots. In each time step, each positioner calls the module that computes the gradient of decentralized navigation function (Table 2). So, the algorithm runs in a for loop as many times as the number of positioner robots. On the other hand, the inner loop that calculates the gradient of the DNF runs constant times (number of adjacent positioners = 6). Therefore the complexity of the algorithm will remain O(N), where N is the number of positioner robots. Considering the fact that all the robots' bases are fixed to the focal plane, collisions can occur locally and chances of collision is only with the certain adjacent robots. Decentralizing motion planning and trajectory generation takes advantage of limited number of adjacent robots and the locality of collisions and significantly reduces the complexity of the algorithm to a linear order. Low complexity of the algorithm guarantees its ease of use in mid-scale and large-scale robotic telescopes where there are thousands, or tens of thousands of positioners respectively.

5. Collision-Free Motion Toward the Equilibrium

The following theorem provides conditions under which the DNF (2) in combination with the control law (3) ensures convergence of all robots to their target points. Convergence of all robots means that using this method, practically no blocking will occur even if some complex maneuvers are needed in case of intricate initial configurations of the robots (See simulation example in Fig. 7).

Theorem 1. *If the following inequality is satisfied:*

$$\frac{\lambda_1}{\lambda_2} < \frac{1}{R}\frac{D}{D^2 - d^2} \tag{5}$$

then the function (2) is a Morse function (Milnor 1963) and there is no local minimum except the equilibrium in the target point.

Proof. When $\nabla_{\theta_i} \psi(q_i) = 0$

It is either in the presence of no other positioner in the vicinity of positioner i, where $\left\| q_i - q_j \right\| \geq D$ or there is a risk of collision $\left\| q_i - q_j \right\| < D$ with at least one other positioner. The gradient of the navigation function for both cases is:

$$\nabla \psi(q_i) = \begin{cases} 2\lambda_1(q_i - q_{iT}) = 0 & \left\| q_i - q_j \right\| \geq D \\ \lambda_1(q_i - q_{iT}) + 2\lambda_2 \sum_{j=1}^{6} \frac{(D^2 - d^2)(q_i - q_j)}{(\left\| q_i - q_j \right\|^2 - d^2)^2} & \left\| q_i - q_j \right\| < D \end{cases} \tag{6}$$

In case when there is no other positioner near the positioner i, $\nabla_{\theta_i} \psi(q_i) = 0$ means $2\lambda_1(q_i - q_{iT}) = 0$, which directly indicates that the positioner robot is in its target point. Otherwise, there is at least one other positioner in the collision avoidance envelope (D):

Table 1. Motion planning algorithm for all positioner robots. T_0 and T_f are the beginning and end times of the algorithm respectively. dt is the time step and M is the number of time steps i.e. $M = \frac{T_f - T_0}{dt}$

Trajectory planning algorithm	
Inputs:	Initial end-effector position of all the positioners: $Q_{init} = [q_1, q_2, \ldots, q_N]$ and target position of all fibers assigned to each positioner: $Q_{goal} = [q_{1T}, q_{2T}, \ldots, q_{NT}]$
outputs:	A sequence of motor peed values for each positioner $\Omega_1 = [\omega_1(1), \ldots, \omega_1(M)]$ $\Omega_2 = [\omega_2(1), \ldots, \omega_2(M)]$ $\vdots$ $\Omega_N = [\omega_N(1), \ldots, \omega_N(M)]$
m = 0	
repeat until $\nabla\psi = 0$	
for each positioner(i=1:N)	
$\omega_i(m) = -\nabla\psi(q_i(m), q_{iT}, Q(m))$ See: Table 2	
$q_i(m+1) = q_i(m+1) + dt.\omega_i(m)$	
m = m + 1	
$\nabla\psi = \max_i(\nabla\psi(q_i(m), q_{iT}, Q(m)))$	
end for	
end repeat	

Table 2. Motion planning algorithm calls this module that calculates gradient of the DNF. This function gets the current and target position of the robot as well as current position of its adjacent positioners. The output of the function is the gradient of the DNF.

Gradient of the DNF for the positioner i	
Inputs:	Current position of the positioner q_i, target position of the positioner q_{iT}, and current position of the neighbor positioners $Q_{neighbor} \in Q$
outputs:	The gradient of the navigation function for positioner i which is a vector of a two elements $G = \begin{pmatrix} G_1 \\ G_2 \end{pmatrix}$
$G = 0$	
$G = G + 2\lambda_1(q_i - q_{iT})$	
for each neighbor positioner(j=1:6)	
$G = G + 2\lambda_2 \frac{(R^2 - r^2)(q_i - q_j)}{(\|q_i - q_j\|^2 - r^2)^2}$	
end for	

$$\nabla\psi(q_i) = \lambda_1(q_i - q_{id}) + 2\lambda_2 \sum_{j=1}^{6} \frac{(D^2 - d^2)(q_i - q_j)}{(\|q_i - q_j\|^2 - d^2)^2} \tag{7}$$

The first term in the gradient of the potential field always satisfies the following inequality:

$$\lambda_1 \|q_i - q_{id}\| < 2\lambda_1 R \tag{8}$$

In addition, the second term in the gradient of the potential field is:

$$\begin{aligned} &\frac{(D^2 - d^2)\|(q_i - q_j)\|}{(\|q_i - q_j\|^2 - d^2)^2} > \frac{D}{D^2 - d^2} \\ &\rightarrow \lambda_2 \sum_{j=1}^{6} \frac{(D^2 - d^2)\|(q_i - q_j)\|}{(\|q_i - q_j\|^2 - d^2)^2} > \lambda_2 \frac{2D}{D^2 - d^2} \end{aligned} \tag{9}$$

So, if $\lambda_2 \frac{2D}{D^2 - d^2} > 2\lambda_1 R$ then there is no point where the gradient of the potential field could be zero except at the target point. It is worth noticing that, there are two possibilities two have velocities equal to zero in angular coordination. One possibility is that the velocities are zero in the (x, y) coordination that is covered in the proof. The other possibility is that the positioner is in one of its singular configurations such as fully stretched or fully bent second arm. Technically, in any robotic manipulation, we try to avoid singularities, as the smoothness of motion and load on the motors are largely affected near singular points. So, we can assure that, in practice, the algorithm can guarantee deadlock-free motion.This guarantees that there will be no blocking (also called deadlock) in the method.

5.1. Parameter tuning

There are two weighting parameters that can be tuned in the DNF (2); λ_1 and λ_2. Theorem 1 gives a condition for tuning this parameters which guarantees convergence of all positioners to their target point. In order to ensure the success of the motion planning algorithm, the maximum velocity generated should not exceed the maximum velocity feasible for motors. Lower values of λ_1 and λ_2 will result in lower values for velocity of motors and increase the convergence time. For an application in which fast convergence is desirable, the two parameters will be tuned to the highest values that still keep maximum generated velocity in the feasible range. We soft-tuned these two parameters through simulations.

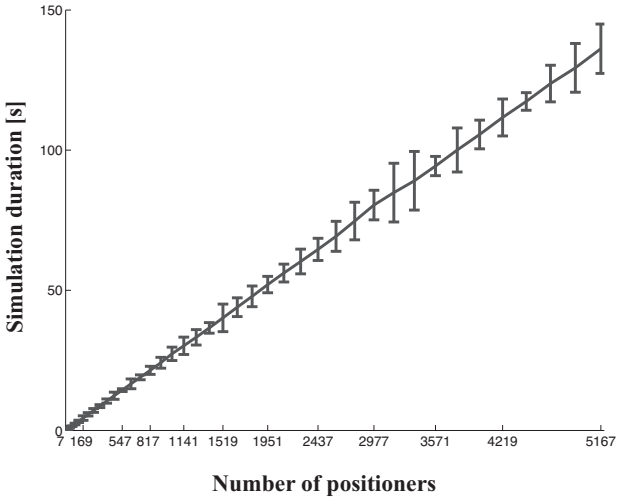

Fig. 5. Mean value simulation duration for sets with different number of positioners. Repeating sets of simulation, the simulation durations do not significantly vary. The lengths of the error bars are therefore chose 10 times of the standard deviation at each point.

6. Simulation Results

In order to study the performance of the motion planning algorithm, we conducted various sets of simulations for different number of positioners all in hexagonal configuration patterns. The size of positioners and the share volume between positioners are selected in a way to be compatible with next-generation spectrograph robots such as the one in DESI (Table 3). Therefor the overlapping area of the robots are the fiber-ends. In a scenario with different specifications, the robots may have collision risks with other parts. In these scenarios, the collision avoidance envelope, D, should be modified in order to cover all collision risks.

For each set of simulations, We selected different numbers of positioners to verify our expectation on complexity of the algorithm. In addition, we can extrapolate the simulation time and motion duration for other number of positioners for larger scales of robotic spectrographs. For each set we repeated the simulations 100 times. In all sets, initial angular position of the two motors of each positioner robot and their target point are randomly generated. Table. 4 shows simulation parameters. The two weighting parameters in DNF (2) should satisfy the condition of Theorem 1. According to positioners' specifications in Table 3, λ_1 and λ_2 should fit the inequality of $\frac{\lambda_1}{\lambda_2} < \frac{1}{R}\frac{D}{D^2-d^2}$. This means $\lambda_1 < 72\lambda_2$.

Table 3. Specifications of positioner robots (see Fig. 3 and Fig. 4)

Parameter	Value
R	7 mm
r	5 mm
ferule size	1 mm
arm diameter	2 mm
arm length	3mm
D	4 mm
d	2 mm

Table 4. Simulation parameters used for all sets of simulations

Parameter	Value
Maximum speed of the first acuator	30 rpm
Maximum speed of the second acuator	20 rpm
λ_1	1
λ_2	0.05
dt (time steps)	10 ms
Convergence distance	100 μm

As expected, we observe no collision during all sets of simulations (4100 sets). Fig. 5 and Fig. 6 show the simulation time and in-motion duration of robots respectively. In-motion duration is the convergence time needed for all the positioner robots to arrive in their target points considering constraints on actuator velocities in Table. 4. Regarding values for simulation time, the processor for all simulations is a 3.33 GHz 6-Core Intel Xeon.

As expected , simulation time increases in a near linear manner with the number of positioners. This enables us to use this method for immediate motion planning for thousands of positioners. From the results, the amount of time needed to generate collision-free trajectories for 5000 positioners is less than 3 minutes (140 seconds) on today's typical computers. This amount of time is very reasonable as it is smaller than the typical exposure time foreseen for the DESI and PFS experiment, thus allowing to have an interactive planning of the observation. This would allow to modify in real time the target list due to many reasons, for example meteorological disturbances or even the last minute discovered transient targets such as SuperNovae or Gamma Ray Burst.

The main advantage of the method that derives from the idea of decentralization is that the motion duration does not change with the number of positioner robots. Decentralization benefits from the configuration of positioner robots and the fact that collisions could happen locally and they do not affect the motion of non-neighbor positioners. With realistic actuator constraints (Table 4), as used in simulation sets, we can expect to accomplished the first run of motion for positioners of a mid-scale robot positioners in less than 2.5 seconds. Such small duration of time for coordination of all positioners will allow to maximize the duration of observation and survey efficiency.

So far, in all sets of simulations, we study the performance of our motion planning algorithm for randomly distributed initial positions and randomly distributed target points. However, galaxies are not randomly distributed, but clustered. Therefore, in a realistic situation, positioners will move toward very close targets and consequently start the next set of observation from a very close position toward other set of target points. Therefore, It is expected that adjacent positioner robots will need sets of complex maneuvers in order to find a collision-free path toward their target points. Fig. 7 shows snap-shots of a simulation set where three positioners are engaged in a very close space. The motion planning algorithm succeeds in solving the conflict by directly executing the complex maneuvers from DNF and taking positioner robots to their target points. The main advantage of this method is that these type of conflicts could be solved in a decentralized manner which significantly decreases simulation time and motion duration. Therefore, the algorithm is reliable for large number of positioners.

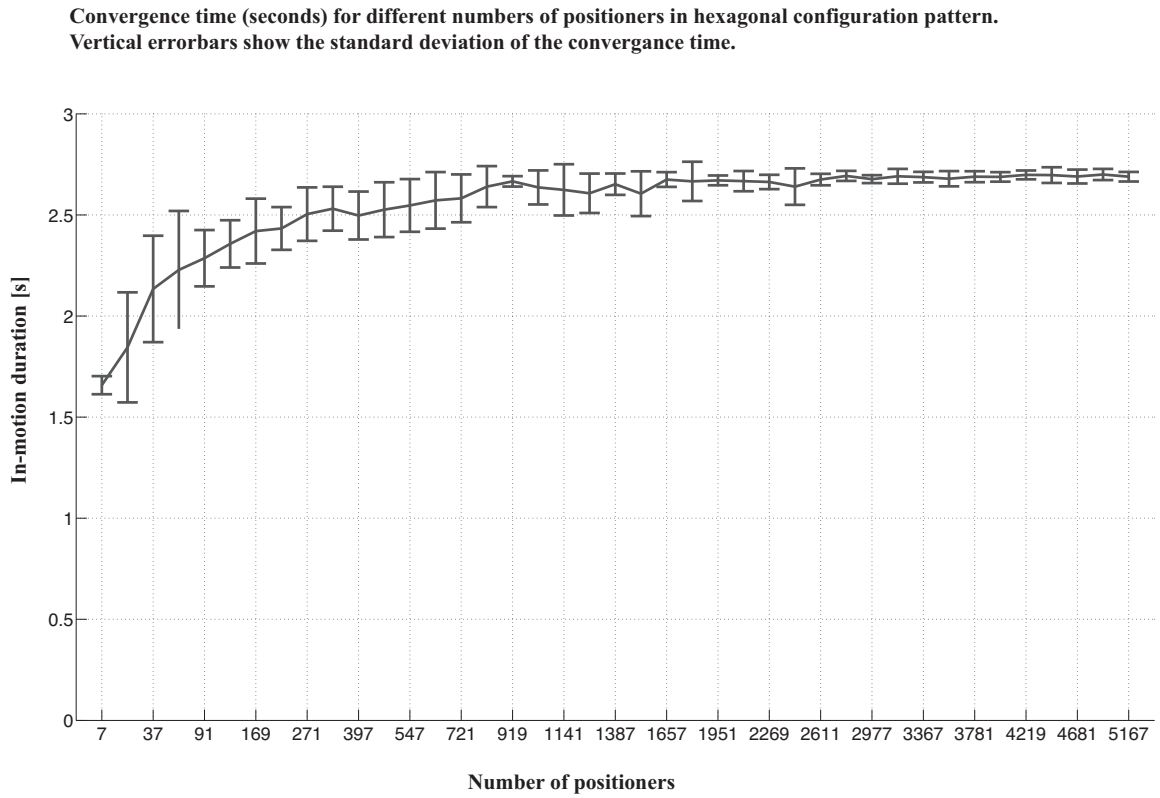

Fig. 6. Mean value and standard deviation of convergence time (seconds) for simulation sets with different numbers of positioners. Note that the scaling of the x-axis is not linear.

7. Conclusion

In the near future fibre-fed spectrograph robots such as the ones envisioned in DESI (5000 positioner robots) or PFS (2400 positioner robots) will provide a 3D map of a large portion of our universe. The main concept which is common between the designs is the use of small mechanical robot positioners. These robot positioners are responsible for moving the fiber-ends toward their target points where they can observe different sets of objects such as galaxies, quasars or stars. As the robot positioners share work-space, the key challenge is designing a motion planning algorithm which guarantees collision avoidance. Our proposed decentralized method for coordination of positioners is a potential field that ensures collision avoidance as well as convergence of positioner robots (no blocking) to their target points. Simulation results show feasibility of using this method for mid-scale and large scale fiber-fed spectrograph robots. In-motion duration only lasts 2.5 seconds for any number of positioners. In addition, the massive spectroscopic projects could take advantage of short simulation time to compute trajectories and the ability of interactive motion planning of the robots to target recently discovered transient sources at the last minute. Granting the fact that the initial motivation of this work came from the collision challenge in DESI project, the proposed method can be directly applied to PFS project where number of robots is half of DESI. From simulation results we can predict that the 4800 trajectories of 2400 robots could be generated with a typical computer in less than one minute and the motion duration would be less than 3 minutes. Moreover, this DNF could be adopted for other fiber positioning systems with different geometry patterns to avoid collisions.

Our future research directions include the discretization of velocity profiles in order to ensure the feasibility of a real-time coordination for large number of positioner robots. In a framework where a centralized computer communicates with positioner robots, in order to minimize the communication time, the motor velocities should be discretized to fit in few bits. Moreover, we are exploring the connection between motion planning and target assignment in order to further minimize the in-motion duration of positioner robots.

Acknowledgements. LM, JPK and LJ acknowledge the support from the European Research Council (ERC) advanced grant "Light on the Dark" (LIDA). FP and JS thanks the support from the Spanish MINECO grants AYA10-21231 and MultiDark-CSD2009-0064.

References

Lauren Anderson, Eric Aubourg, Stephen Bailey, Dmitry Bizyaev, Michael Blanton, Adam S Bolton, J Brinkmann, Joel R Brownstein, Angela Burden, Antonio J Cuesta, et al. The clustering of galaxies in the sdss-iii baryon oscillation spectroscopic survey: baryon acoustic oscillations in the data release 9 spectroscopic galaxy sample. *Monthly Notices of the Royal Astronomical Society*, 427(4):3435–3467, 2012.

Chris Blake, Eyal A Kazin, Florian Beutler, Tamara M Davis, David Parkinson, Sarah Brough, Matthew Colless, Carlos Contreras, Warrick Couch, Scott Croom, et al. The wigglez dark energy survey: mapping the distance–redshift relation with baryon acoustic oscillations. *Monthly Notices of the Royal Astronomical Society*, 418(3):1707–1724, 2011.

Xiangqun Cui, Shou-guan Wang, Ding-qiang Su, Yongheng Zhao, Ya-nan Wang, Yaoquan Chu, and Guoping Li. Southern lamost for all sky spectroscopic survey. In *SPIE Astronomical Telescopes and Instrumentation: Observational Frontiers of Astronomy for the New Decade*, pages 77330B–77330B. International Society for Optics and Photonics, 2010.

Maria Carmela De Gennaro and Ali Jadbabaie. Formation control for a cooperative multi-agent system using decentralized navigation functions. In *American Control Conference, 2006*, pages 6–pp. IEEE, 2006.

Dimos V Dimarogonas and Kostas J Kyriakopoulos. Decentralized motion control of multiple agents with double integrator dynamics. In *16th IFAC World Congress, to appear*, 2005.

G Efstathiou, WJ Sutherland, and SJ Maddox. The cosmological constant and cold dark matter. *Nature*, 348(6303):705–707, 1990.

Daniel J Eisenstein, Idit Zehavi, David W Hogg, Roman Scoccimarro, Michael R Blanton, Robert C Nichol, Ryan Scranton, Hee-Jong Seo, Max Tegmark, Zheng Zheng, et al. Detection of the baryon acoustic peak in the large-scale correlation function of sdss luminous red galaxies. *The Astrophysical Journal*, 633(2):560, 2005.

Fangzhen Ge, Zhen Wei, Yang Lu, Yiming Tian, and Lixiang Li. Decentralized coordination of autonomous swarms inspired by chaotic behavior of ants. *Nonlinear Dynamics*, 70(1):571–584, 2012.

John Huchra, Marc Davis, David Latham, and J Tonry. A survey of galaxy redshifts. iv-the data. *The Astrophysical Journal Supplement Series*, 52:89–119, 1983.

Masahiko Kimura, Toshinori Maihara, Kouji Ohta, Fumihide Iwamuro, Sigeru Eto, Masafumi Lino, Daisaku Mochida, Takanori Shima, Hiroshi Karoji, Junichi Noumaru, et al. Fibre-multi-object spectrograph (fmos) for subaru telescope. In *Astronomical Telescopes and Instrumentation*, pages 974–984. International Society for Optics and Photonics, 2003.

Laleh Makarem and Denis Gillet. Decentralized coordination of autonomous vehicles at intersections. In *World Congress*, volume 18, pages 13046–13051, 2011.

Laleh Makarem and Denis Gillet. Fluent coordination of autonomous vehicles at intersections. In *Systems, Man, and Cybernetics (SMC), 2012 IEEE International Conference on*, pages 2557–2562. IEEE, 2012.

John Milnor. Morse theory, volume 51 of annals of mathematics studies. *Princeton, NJ, USA*, 1963.

Isaac Morales, Antonio D Montero-Dorta, Marco Azzaro, Francisco Prada, Justo Sánchez, and Santiago Becerril. Fibre assignment in next-generation wide-field spectrographs. *Monthly Notices of the Royal Astronomical Society*, 419 (2):1187–1196, 2012.

Saul Perlmutter, G Aldering, G Goldhaber, RA Knop, P Nugent, PG Castro, S Deustua, S Fabbro, A Goobar, DE Groom, et al. Measurements of ω and λ from 42 high-redshift supernovae. *The Astrophysical Journal*, 517(2):565, 1999.

Adam G Riess, Alexei V Filippenko, Peter Challis, Alejandro Clocchiatti, Alan Diercks, Peter M Garnavich, Ron L Gilliland, Craig J Hogan, Saurabh Jha, Robert P Kirshner, et al. Observational evidence from supernovae for an accelerating universe and a cosmological constant. *The Astronomical Journal*, 116(3):1009, 1998.

Herbert G Tanner and Amit Kumar. Towards decentralization of multi-robot navigation functions. In *Robotics and Automation, 2005. ICRA 2005. Proceedings of the 2005 IEEE International Conference on*, pages 4132–4137. IEEE, 2005.

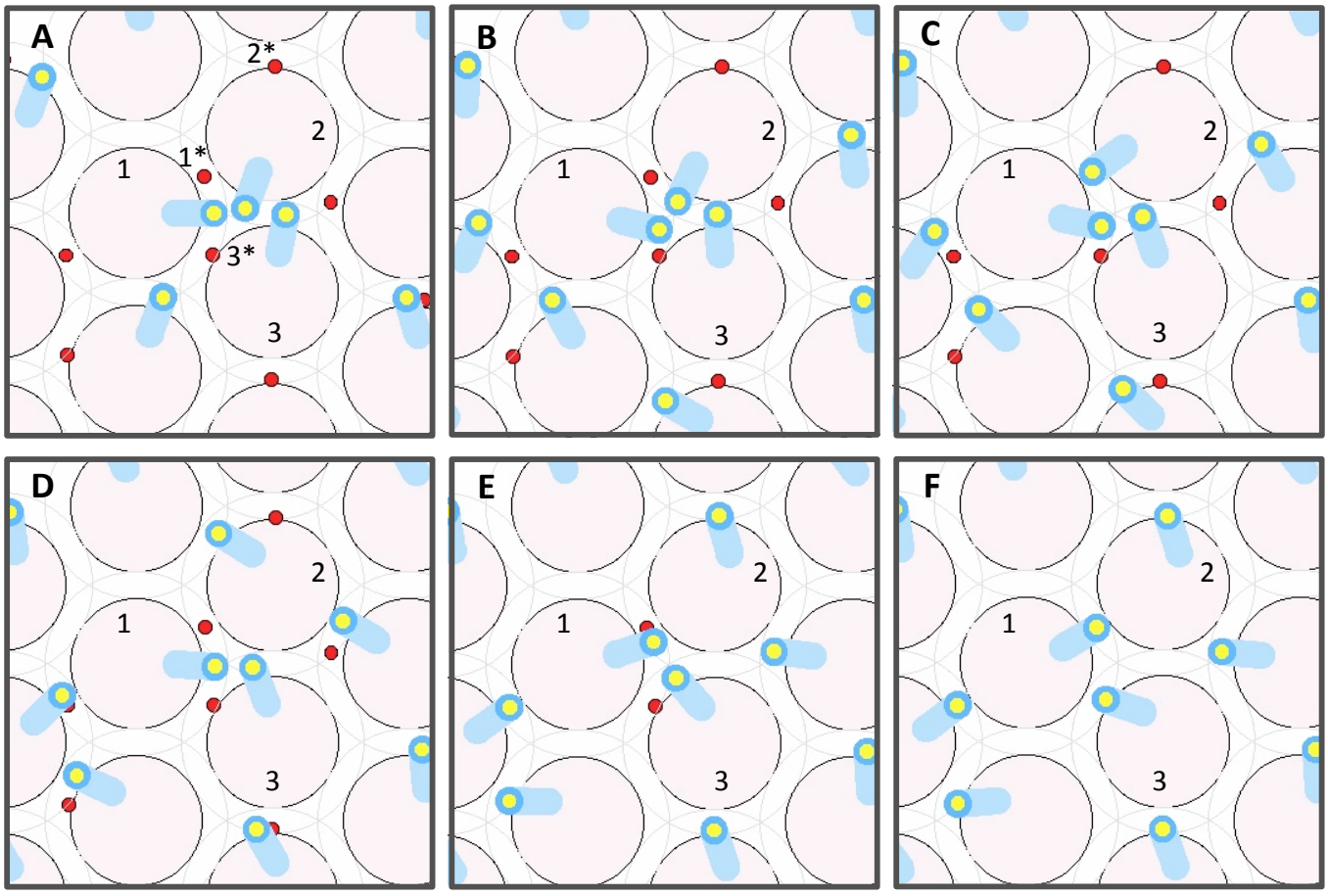

Fig. 7. The six boxes (A to F) show six snap shots of the simulation. 1*, 2* and 3* are respectively the target positions for positioner 1,2 and 3. This three positioners are engaged in a local conflict in which positioner 1 needs to make space for positioner 2 to pass. positioner 2 can not make room for positioner 1 because positioner 3 is blocking the way. Positioner 3 needs to pass both positioners to reach its target point. The small maneuver from positioner 1 that comes directly from DNF moves this positioner farther from its target point but it makes room for the positioner 2 to pass safely. When positioner 2 clears the way, positioner 1 starts moving toward its target point and this gives a safe way to the positioner 3.

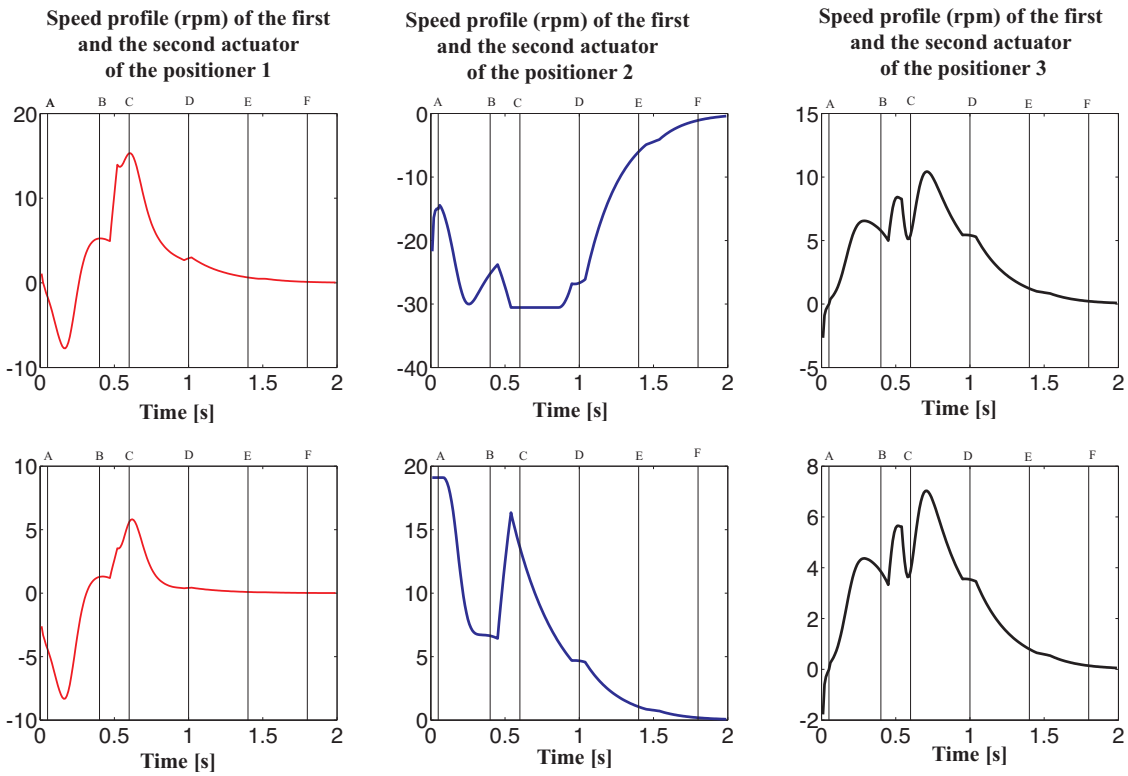

Fig. 8. Velocity profiles that correspond to the pairs of actuators for positioners 1,2 and 3 in Fig. 7. Columns show the velocity profiles for each positioner. The first and second profiles of each column correspond to the first and second actuator of each positioner respectively. Vertical lines indicate the moment at which the snapshots of Fig. 7 were taken.